

Severely reduced neutrophil adhesion and impaired host defense against fecal and commensal bacteria in CD18^{-/-}-P-selectin^{-/-} double null mice

STEPHEN BRADLEY FORLOW,^{*,†} PATRICIA L. FOLEY,[‡] AND KLAUS LEY^{*,†,1}

^{*}Department of Biomedical Engineering, [†]Cardiovascular Research Center, and [‡]Center for Comparative Medicine, University of Virginia, Charlottesville, Virginia, USA

ABSTRACT Leukocyte recruitment to sites of inflammation requires the functions of selectins and integrins. P-selectin null (CD62P^{-/-}) mice show a mild and CD18 null (CD18^{-/-}) mice a more severe neutrophil recruitment defect in some inflammatory models. To investigate the possible cooperative interactions between CD18 integrins and P-selectin in mediating neutrophil recruitment, we generated CD18^{-/-}-CD62P^{-/-} double null mice. CD18^{-/-}-CD62P^{-/-} mice were apparently normal at weaning and fertile but later failed to gain weight, showed increased susceptibility to infection by fecal and commensal bacteria, and survived only 5–6 months. Some CD18^{-/-}-CD62P^{-/-} mice showed severe spontaneous skin lesions; most showed neutrophil infiltration in the lungs and liver, and positive bacterial cultures from internal organs. The number and velocity of rolling leukocytes in tumor necrosis factor α treated venules of CD18^{-/-}-CD62P^{-/-} mice was similar to those in wild-type mice, but neutrophil adhesion was severely reduced. Only 25% of adhered leukocytes were neutrophils in CD18^{-/-}-CD62P^{-/-} mice vs. >90% in wild-type, CD62P^{-/-}, and CD18^{-/-} single mutants. Our data show that removing both P-selectin and CD18 integrins from mice leads to severe neutrophil recruitment defects and spontaneous pathology.—Forlow, S. B., Foley, P. L., Ley, K. Severely reduced neutrophil adhesion and impaired host defense against fecal and commensal bacteria in CD18^{-/-}-P-selectin^{-/-} double null mice. *FASEB J.* 16, 1488–1496 (2002)

Key Words: integrins • knockout • intravital microscopy • inflammation • adhesion molecules

LEUKOCYTE RECRUITMENT to inflammatory sites occurs through a multistep process that involves the selectin, integrin, and immunoglobulin families of adhesion molecules. Initial capture (tethering) and rolling of leukocytes on activated endothelial cells are largely mediated by the selectins (L-, P-, and E-) and their ligands (1, 2). Rolling leukocytes may become activated by surface-bound chemokines that promote β_2 integrin-dependent firm adhesion. Recent evidence shows that L- and E-selectin ligation can also signal the up-regulation of adhesion events through β_2 integrins in vitro

(3–6) and in vivo (3). Together, these activating signals lead to firm arrest of slowly rolling leukocytes (7, 8).

Elevated leukocyte rolling velocities result when CD18 integrin function is blocked or absent, suggesting that CD18 integrins act synergistically with P- and E-selectin to stabilize leukocyte rolling (7, 9, 10). Slow leukocyte rolling requires both CD18 integrins and E-selectin and is a critical aspect of the leukocyte recruitment cascade that enables leukocytes to transition from rolling to firm adhesion (9, 10). In a previous study, we generated mice lacking both CD18 integrins and E-selectin and found significantly elevated leukocyte rolling velocities (>50 $\mu\text{m/s}$), resulting in a drastic reduction of neutrophil adhesion (10). As a result of the dramatic neutrophil recruitment defect, CD18^{-/-}-CD62E^{-/-} mice generally did not survive to weaning (10). These data show that CD18 integrins and E-selectin cooperatively mediate slow rolling, which allows the conversion of rolling to firm adhesion and represents a bottleneck in the adhesion cascade (8).

P-selectin is a type I integral membrane protein composed of a C-type lectin domain, an epidermal growth factor-like domain, a series of short consensus-repeat domains, a transmembrane domain, and a short cytoplasmic tail (2). P-selectin expression is induced on endothelial cells in response to various inflammatory mediators (2). The main ligand for P-selectin is P-selectin glycoprotein ligand 1 (PSGL-1), which is constitutively expressed on circulating leukocytes (11, 12). The binding of P-selectin to PSGL-1 is the primary mechanism by which circulating leukocytes tether to and roll on activated endothelial cells (13). Mice lacking P-selectin show a 50% reduction in the number of rolling leukocytes (rolling flux), resulting in ~50% fewer firmly adhered leukocytes in a cytokine-induced model of inflammation (14).

The β_2 (CD18) integrins are heterodimeric molecules composed of an α chain (CD11a, b, c, or d) and a common β chain. Although CD18 integrins are thought to be a predominant neutrophil adhesion mechanism in acute inflammation, CD18^{-/-} mice

¹ Correspondence: Department of Biomedical Engineering, Health Sciences Center Box 800759, Charlottesville, VA 22908, USA. E-mail: klausley@virginia.edu

display neutrophil adhesion levels that are not different from wild-type mice in a tumor necrosis factor α (TNF- α)-induced model of inflammation of the mouse cremaster muscle (9). This is partially due to a compensatory increase in circulating neutrophil numbers that are \sim 10- to 20-fold elevated (15). To understand possible cooperative interactions of CD18 integrins and P-selectin in neutrophil recruitment, we generated mice lacking both CD18 integrins and P-selectin. These mice show a very severe neutrophil recruitment defect (much more so than CD18 single mutant mice), colonization of several organs with commensal bacteria, severe lung pathology, and premature death.

EXPERIMENTAL PROCEDURES

Generation of CD18^{-/-}CD62P^{-/-} double mutant mice

Mice deficient in CD18 and P-selectin were generated by cross-breeding CD18^{-/-} C57BL/6 N6 (15) and P-selectin^{-/-} C57BL/6 N6 (16) mutants. Homozygosity of the double mutants was confirmed by PCR for wild-type and mutant alleles (data not shown). For some intravital microscopy experiments, CD18^{-/-} and CD18^{-/-}CD62P^{-/-} mice were generated by transplanting CD18^{-/-} bone marrow into lethally irradiated wild-type or CD62P^{-/-} mice as described previously (17). Since data in intravital microscopy experiments from null mice were indistinguishable from data obtained from mice generated by transplantation, these data were pooled.

Intravital microscopy

Mice were anesthetized with an intraperitoneal (i.p.) injection of ketamine hydrochloride (Ketalar, 125 mg/kg; Parke-Davis, Morris Plains, NJ), xylazine (12.5 mg/kg; Vedco, Inc., St. Joseph, MO), and atropine (0.25 mg/kg; Elkins-Sinn, Inc., Cherry Hill, NJ) and prepared for intravital microscopy as described (10). Recombinant murine TNF- α (Genzyme, Cambridge, MA) was injected intrascrotally at a dose of 500 ng per mouse in a volume of 0.3 mL of sterile saline 2 h before exteriorization of the cremaster muscle. For some experiments, wild-type mice were administered an anti-P-selectin mAb RB40.34 (100 μ g i.p.; ref 18), an anti-CD18 integrin mAb GAME-46 (100 μ g i.p.; PharMingen, San Diego, CA), or both RB40.34 and GAME-46. To facilitate the counting of adherent leukocytes in some experiments, all leukocyte rolling was blocked with an anti-E-selectin mAb [9A9, 30 μ g intravenous (i.v.)] (19) and/or an anti-P-selectin mAb [RB40.34; 30 μ g i.v.] 75 min after exteriorization of the cremaster muscle. The number of leukocytes that remained adhered were counted and expressed as per unit area. Systemic leukocyte counts and differentials were obtained from blood samples collected from the carotid artery at 2 h post-TNF- α treatment (before exteriorization of cremaster muscle) and at \sim 3.5 h post-TNF- α treatment (completion of experiment).

Rolling and adhesion parameters

A digital image processing system was used to measure microvessel diameters, lengths, (20), and leukocyte rolling velocities (21). To determine whether CD18 integrins and P-selectin function cooperatively to mediate leukocyte cap-

ture/rolling or stable leukocyte rolling, leukocyte rolling flux and leukocyte rolling velocity were measured. Leukocyte rolling flux, expressed as leukocytes per minute, was calculated by counting leukocytes rolling past a line perpendicular to the vessel axis. The number of rolling leukocytes (rolling flux) is indicative of the ability of circulating leukocytes to tether to and roll on activated endothelial cells (initiation of leukocyte recruitment). Leukocyte rolling is a prerequisite for firm adhesion; however, slow leukocyte rolling (<10 μ m/s) is necessary for efficient conversion from rolling to firm adhesion (10). Leukocyte rolling velocities were measured for 10 leukocytes per venule. Adherent leukocytes were defined as leukocytes that did not move for at least 30 s. The total number of adhered leukocytes was determined for each venule segment (\sim 200 μ m) and expressed per unit area (of inside surface area of the vessel). Leukocyte adhesion differentials were determined by multiplying the intravascular differential counts obtained by histology with the leukocyte adhesion density obtained by intravital microscopy. Neutrophil adhesion efficiency, defined as the ability of circulating neutrophils to become adherent, was calculated by dividing the number of adhered neutrophils per unit area by the concentration of neutrophils in the systemic circulation.

Histology

To differentiate intravascular and interstitial leukocytes, cremaster muscle whole mounts were prepared as described previously (9). The Giemsa-stained cremaster muscles were observed by using a Zeiss microscope with a 100 \times , 1.4 numerical aperture oil immersion objective (Zeiss, Oberkochen, Germany). Intravascular and interstitial leukocytes were counted and differentiated into neutrophils, eosinophils, and mononuclear cells. The interstitial tissue observed was a circular area (diameter of 183 μ m) bisected by each venule. To assess potential inflammatory lesions in other organs, wild-type and age-matched CD62P^{-/-}, CD18^{-/-}, and CD18^{-/-}CD62P^{-/-} mice were analyzed for gross and microscopic pathology. Lung, liver, spleen, heart, kidney, gut, and skin samples were fixed in 10% buffered formalin (Sigma Chemical Co., St. Louis, MO), embedded in paraffin, and examined after hematoxylin and eosin staining.

Microbiological analyses

Tissue samples for microbiologic analysis were obtained in sterile fashion from the lung, liver, and spleen from wild-type, CD62P^{-/-}, CD18^{-/-}, and CD18^{-/-}CD62P^{-/-} mice. Tissues were homogenized with a sterile grinder in 0.5 mL PBS. A 100 microliter sample from each tissue was plated onto trypticase soy agar with 5% sheep red blood cells (Difco, Detroit, MI). Plates were observed at 24 and 48 h for growth. Individual representative colonies from samples that were positive for growth were gram-stained and sent to a clinical microbiology laboratory for further identification (Clinical Microbiology, University of Virginia).

Statistics

Student's *t*-Test and Mann-Whitney Rank Sum Test were used to determine statistically significant differences of body weights among mouse strains. Average leukocyte rolling velocities, leukocyte adhesion, leukocyte rolling flux, and leukocyte differentials between groups were compared by using Kruskal-Wallis 1-way ANOVA on ranks and pairwise multiple comparison by Dunn's method. Statistical significance was set at $P < 0.05$.

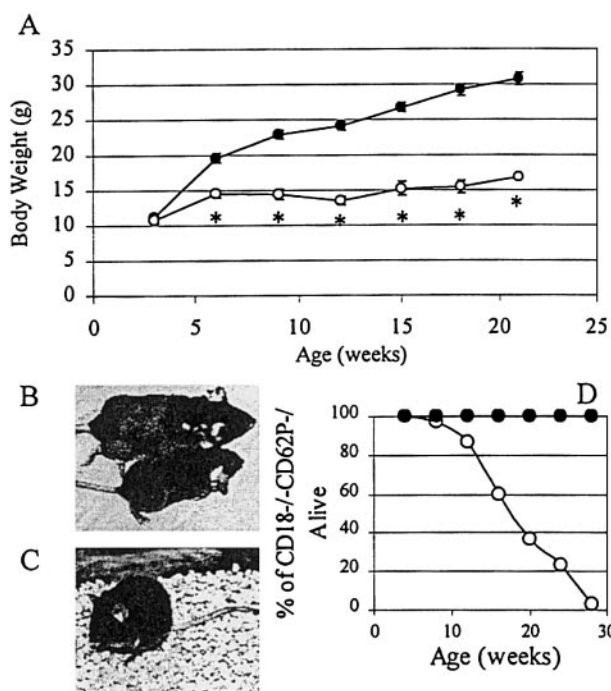


Figure 1. Growth curve of mice deficient in CD18 integrins and P-selectin. *A*) CD18^{-/-}CD62P^{-/-} double mutant mice (open circles) have the same body weights as CD18^{+/+}CD62P^{-/-} littermates (filled circles) at weaning (3 wk). However, CD18^{-/-}CD62P^{-/-} mice gain minimal weight after 5 wk and remain significantly smaller than littermates 6–21 wk of age. *Significantly different from CD18^{+/+}CD62P^{-/-} mice at 6–21 wk ($P < 0.001$). Data expressed as mean \pm SE. *B*) CD18^{-/-}CD62P^{-/-} are significantly smaller than CD18^{+/+}CD62P^{-/-} littermates in adulthood (males, 15 wk old). *C*) CD18^{-/-}CD62P^{-/-} mice showed dramatic weight loss and became severely hunched preceding death (female at 15 wk, 9.9 g). *D*) CD18^{-/-}CD62P^{-/-} mice show drastically reduced viability after weaning. ~60% of the colony died or was killed in accordance with IACUC procedures by ~20 wk of age. Only 1 CD18^{-/-}CD62P^{-/-} mouse of 30 survived > 6 months. No deaths in CD18^{+/+}CD62P^{-/-} mice (filled circles).

RESULTS

Phenotype of CD18^{-/-}CD62P^{-/-} mice

CD18^{-/-}CD62P^{-/-} double mutant mice produced from CD18^{+/+}CD62P^{-/-} breeders were indistinguishable from littermate controls at birth through weaning.

The weaning weight of CD18^{-/-}CD62P^{-/-} mice was 10.7 ± 0.4 g ($n=17$) compared with 11.2 ± 0.3 g for CD18^{+/+}CD62P^{-/-} and CD18^{+/+}CD62P^{-/-} littermates ($n=64$) (Fig. 1A, 3 wk). As we reported previously (10), young CD18^{-/-}CD62P^{-/-} mice were fertile and able to produce live offspring. However, CD18^{-/-}CD62P^{-/-} mice failed to gain weight after 5 wk and developed a more severe phenotype than either CD18^{-/-} or CD62P^{-/-} single mutant mice. Some CD18^{-/-}CD62P^{-/-} mice developed the characteristic facial ulcerative dermatitis or conjunctivitis seen in CD18^{-/-} mice (15). Most CD18^{-/-}CD62P^{-/-} mice that developed skin lesions displayed severe ulcerative dermatitis on the neck and contracture of the submandibular soft tissue. CD18^{-/-}CD62P^{-/-} mice were significantly smaller than littermates in adulthood (Fig. 1B), showing only minimal weight gain after weaning, although they were active and eating (Fig. 1A; $P < 0.001$). The body weight data represent a somewhat healthier population of mice because severely sick mice died or were killed throughout the experiment. Before death, these mice became severely hunched and often weighed < 10 g (Fig. 1C). Although apparently healthy after birth, ~40% of the CD18^{-/-}CD62P^{-/-} mice died by 16 wk of age (Fig. 1D). Only 1 of 30 CD18^{-/-}CD62P^{-/-} mice survived past 24 wk. Neither CD18^{-/-} nor CD62P^{-/-} single mutant mice show reduced viability within 6 months of birth (refs 14, 15 and data not shown).

Intravital microscopy

Based on the premature lethality of CD18^{-/-}CD62P^{-/-} mice, we hypothesized that eliminating both CD18 integrins and P-selectin function might severely impair neutrophil recruitment to sites of inflammation. We investigated leukocyte rolling and adhesion in hemodynamically similar venules (Table 1) in wild-type, CD62P^{-/-}, CD18^{-/-}, and CD18^{-/-}CD62P^{-/-} mice in venules of TNF α -treated cremaster muscle. Removing P-selectin function reduced the leukocyte rolling flux to 25 ± 5 leukocytes/min vs. 79 ± 11 leukocytes/min in wild-type mice (Fig. 2A). Leukocyte rolling flux was significantly elevated to 262 ± 42 leukocytes/min in CD18^{-/-} mice compared with wild-type and CD62P^{-/-} mice (Fig. 2A). The increased leukocyte rolling flux most likely results from elevated circulating neutrophil counts (Fig. 2B,

TABLE 1. Hemodynamic data and systemic leukocyte counts in TNF α -treated mice^a

	Wild-type	CD62P ^{-/-}	CD18 ^{-/-}	CD18 ^{-/-} CD62P ^{-/-}
Number of mice (N)	7	5	4	8
Number of venules (n)	75	37	39	61
Average venule diameter (μ m)	40 ± 2	44 ± 3	44 ± 3	47 ± 2
Average wall shear rate (s^{-1})	665 ± 44	475 ± 42	493 ± 33	615 ± 41
Systemic leukocyte counts (cells/ μ l)	5800 ± 900	5300 ± 1300	$31,100 \pm 9200^b$	$34,200 \pm 7400^b$
Neutrophil counts (cells/ μ l)	1700 ± 300	1500 ± 200	$22,300 \pm 8300^b$	$24,000 \pm 5900^b$
Mononuclear cell counts (cells/ μ l)	4100 ± 900	3900 ± 200	8800 ± 1100^c	$10,200 \pm 1800^c$

^a All values expressed as mean \pm SE. CD62P^{-/-} group ($P < 0.05$).

^b Significantly different from wild-type and CD62P^{-/-} groups.

^c Significantly different from

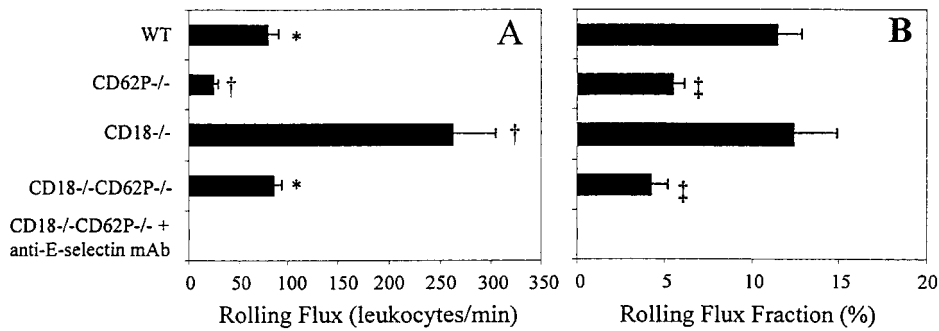


Figure 2. Leukocyte rolling in TNF- α -treated cremaster muscle venules of wild-type, CD62P $^{-/-}$, CD18 $^{-/-}$, and CD18 $^{-/-}$ -CD62P $^{-/-}$ mice. *A*) Leukocyte rolling flux (number of rolling cells per min) was obtained from 37–75 venules. *B*) Leukocyte rolling flux fraction (rolling cells as percentage of all circulating cells in the same vessel). Rolling in CD18 $^{-/-}$ -CD62P $^{-/-}$ mice was completely removed by administration of an anti-E-selectin monoclonal antibody. *Significantly different from CD62P $^{-/-}$ and CD18 $^{-/-}$ groups. †Significantly different from all other groups. ‡Significantly different from wild-type and CD18 $^{-/-}$ groups ($P < 0.05$). Data expressed as mean \pm SE.

CD62P $^{-/-}$ and CD18 $^{-/-}$ groups. †Significantly different from all other groups. ‡Significantly different from wild-type and CD18 $^{-/-}$ groups ($P < 0.05$). Data expressed as mean \pm SE.

Table 1). CD18 $^{-/-}$ -CD62P $^{-/-}$ mice showed a leukocyte rolling flux of 86 ± 7 leukocytes/min, 67% lower than CD18 $^{-/-}$ mice but similar to wild-type mice (Fig. 2A). This number must also be seen in the context of elevated circulating neutrophil counts in CD18 $^{-/-}$ -CD62P $^{-/-}$ mice (Table 1). All leukocyte rolling in CD18 $^{-/-}$ -CD62P $^{-/-}$ mice was eliminated after the administration of an anti-E-selectin antibody (Fig. 2A, B).

The majority of leukocytes in wild-type mice rolled at velocities $< 10 \mu\text{m/s}$ (71%), resulting in an average leukocyte rolling velocity of $8.4 \pm 0.2 \mu\text{m/s}$ (Fig. 3A). A further decrease in average leukocyte rolling velocity occurred in CD62P $^{-/-}$ mice ($4.5 \pm 0.2 \mu\text{m/s}$), because rolling in these mice is E-selectin-mediated (Fig. 3B). In CD18 $^{-/-}$ mice, leukocyte rolling velocities ranged up to $85 \mu\text{m/s}$ and increased the average rolling velocity to $20.9 \pm 0.8 \mu\text{m/s}$ (Fig. 3C). CD18 $^{-/-}$ -CD62P $^{-/-}$ mice showed a leukocyte rolling velocity distribution similar to CD18 $^{-/-}$ mice, but the velocity shift was less severe, reflecting the net sum of reduced rolling velocity in CD62P $^{-/-}$ mice and increased rolling velocity in CD18 $^{-/-}$ mice. The average leukocyte rolling velocity in CD18 $^{-/-}$ -CD62P $^{-/-}$ mice was $15.8 \pm 0.5 \mu\text{m/s}$ (Fig. 3D). These data show that E-selectin can mediate slow leukocyte rolling in the absence of P-selectin and CD18 integrin function, although less efficiently and at higher velocities than when CD18 integrin function is present (in CD62P $^{-/-}$ mice).

Leukocyte adhesion was modestly decreased in CD62P $^{-/-}$ mice (237 ± 29 adherent leukocytes/ mm^2) compared with wild-type mice (402 ± 35 adherent leukocytes/ mm^2). Leukocyte adhesion levels in CD18 $^{-/-}$ mice were similar to those in wild-type mice (500 ± 57 adherent leukocytes/ mm^2), consistent with previous findings (9). CD18 $^{-/-}$ -CD62P $^{-/-}$ mice also displayed similar leukocyte adhesion levels (523 ± 46 adherent leukocytes/ mm^2), suggesting that CD18-independent adhesion of some white blood cells occurs in these mice. However, inspection of leukocyte differentials in Giemsa-stained cremaster whole mounts revealed a selective impairment of neutrophil adhesion in CD18 $^{-/-}$ -CD62P $^{-/-}$ mice. Intravascular and transmigrated neutrophils accounted for only 25% and 12% of all white blood cells, respectively, in CD18 $^{-/-}$ -CD62P $^{-/-}$

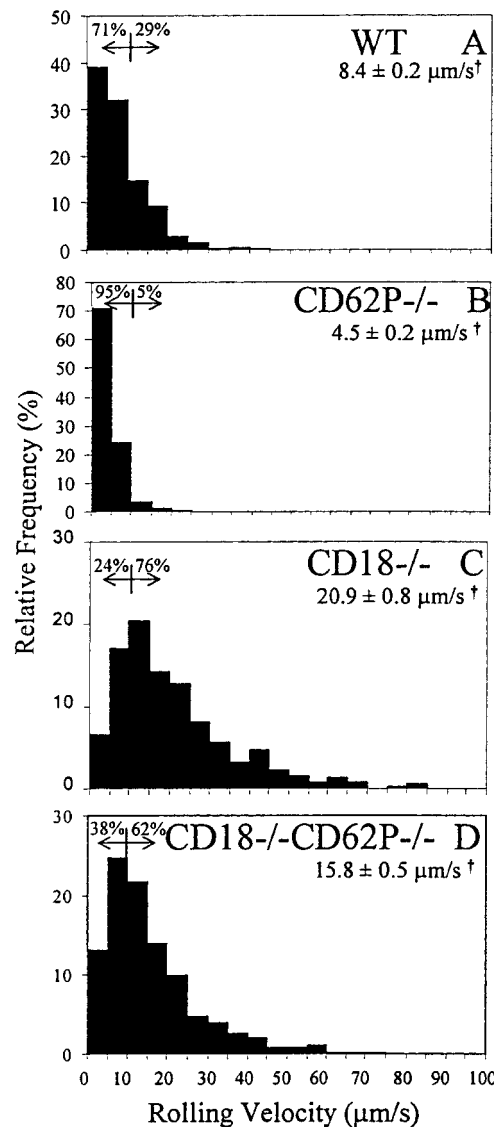


Figure 3. Leukocyte rolling velocity distributions in TNF- α -treated cremaster muscle venules of wild-type, CD62P $^{-/-}$, CD18 $^{-/-}$, and CD18 $^{-/-}$ -CD62P $^{-/-}$ mice. Rolling velocities were obtained from 696 cells in wild-type (A), 333 cells in CD62P $^{-/-}$ (B), 386 cells in CD18 $^{-/-}$ (C), and 628 cells in CD18 $^{-/-}$ -CD62P $^{-/-}$ (D) mice. †Significantly different from all other groups ($P < 0.05$). Average leukocyte rolling velocities expressed as mean \pm SE.

mice vs. > 90% in wild-type, CD62P^{-/-}, and CD18^{-/-} mice (Table 2). The low number of adherent and transmigrated neutrophils point to a severe neutrophil recruitment defect in the absence of CD18 integrins and P-selectin (Table 2). To demonstrate the effect of removing both CD18 integrins and P-selectin on neutrophil recruitment, the number of adherent neutrophils per unit surface area of vessel (Fig. 4A) was calculated from differential counts obtained by histology (Table 2) and the number of adherent leukocytes per unit area obtained by intravital microscopy. The level of neutrophil adhesion is significantly reduced in CD18^{-/-}CD62P^{-/-} mice compared with CD18^{-/-} mice despite equivalent numbers of circulating neutrophils, indicating a prominent role for P-selectin in CD18-independent neutrophil adhesion. These results must be considered in relation to the circulating neutrophil levels in CD18^{-/-}CD62P^{-/-} mice, which are 20-fold higher than CD62P^{-/-} mice. Normalizing neutrophil adhesion levels (cells per mm²) by the circulating neutrophil counts (cells/ μ l) reflect overall neutrophil adhesion efficiency (9). Neutrophil adhesion efficiency is drastically reduced in the absence of both CD18 integrins and P-selectin (Fig. 4B), showing that the CD18-independent component of neutrophil adhesion seen in CD18^{-/-} mice fails in the absence of P-selectin.

To confirm the role of CD18 integrins and P-selectin in neutrophil adhesion in wild-type mice, we administered an anti-P-selectin monoclonal antibody (RB40.34), an anti-CD18 integrin monoclonal antibody (GAME-46), or an anti-CD18 integrin and an anti-P-selectin monoclonal antibody. To accurately count the number of adherent leukocytes, all leukocyte rolling was blocked by the administration of an anti-E-selectin mAb and/or an anti-P-selectin mAb before the tissue was fixed and harvested. Blocking P-selectin or CD18 integrin function significantly reduced leukocyte adhesion (414 \pm 41 adherent leukocytes/mm² and 545 \pm 40 adherent leukocytes/mm², respectively) compared with wild-type mice (938 \pm 47 adherent leukocytes/mm²). Leukocyte adhesion was more severely reduced when both P-selectin and CD18 integrin function was blocked (376 \pm 45 adherent leukocytes/mm²). Leukocyte adhesion differentials confirm the cooperative function of CD18 integrins and P-selectin on neutrophil adhesion. Only 34.5% and 25.1% of adherent and

transmigrated leukocytes, respectively, were neutrophils in wild-type mice when CD18 integrin and P-selectin function was blocked (Table 3). To show the impairment of neutrophil adhesion in wild-type mice lacking both CD18 integrin and P-selectin function, the number of adhered neutrophils per unit area was calculated by multiplying the neutrophil differential obtained from histology (Table 3) by the leukocyte adhesion density obtained by intravital microscopy. The number of adhered neutrophils in mice pretreated with an anti-CD18 integrin and an anti-P-selectin mAb (130 \pm 15 adherent neutrophils/mm²) was reduced compared with untreated wild-type mice (704 \pm 36 adherent neutrophils/mm²) and wild-type mice pretreated with an anti-CD18 mAb (425 \pm 31 adherent neutrophils/mm²) or an anti-P-selectin mAb (248 \pm 24 adherent neutrophils/mm²) (Fig. 4C).

Histopathology

CD18^{-/-}CD62P^{-/-} mice displayed severe and consistent inflammatory lesions in the submandibular region, spleen, lung, and liver. The submandibular/neck lesions are consistent with a chronic active inflammatory process. Neck lesions showed a dramatic loss of epidermis (Fig. 5B) compared with normal skin (Fig. 5A). However, as reported in CD18^{-/-} mice (15), there was a remarkable absence of neutrophils from these areas (Fig. 5C) despite the presence of large bacterial colonies. Lymphocytes and plasma cells, macrophages, and mast cells were all prevalent in the dermis (Fig. 5C).

The spleen of CD18^{-/-}CD62P^{-/-} mice showed a profound expansion of red pulp with neutrophils, plasma cells, and immature mononuclear cells (Fig. 5E), consistent with extramedullary hematopoiesis. This resulted in an ~threefold increase in spleen weight (0.30 \pm 0.07 g) compared with wild-type mice (0.11 \pm 0.01 g), although not different from CD18^{-/-} mice (0.28 \pm 0.04 g). Wild-type mice showed prominent areas of white pulp (Fig. 5D). The white pulp primarily consisted of mature lymphocytes with occasional germinal centers.

The lung pathology in the CD18^{-/-}CD62P^{-/-} mice was dramatic and probably contributed to the clinical demise of these mice. CD18^{-/-}CD62P^{-/-} mice showed vast interstitial neutrophilia throughout the

TABLE 2. Intravascular and transmigrated neutrophils after TNF α treatment^a

	Intravascular differential, % PMN	Average number of PMN inside vessel ^d	Transmigrated differential average number of PMN	
			% PMN	Outside vessel/FOV
Wild-type	92.6 \pm 0.4	57.5 \pm 3.2	90.1 \pm 1.5	11.8 \pm 1.0
CD62P ^{-/-}	91.2 \pm 1.7	35.8 \pm 5.8	79.1 \pm 1.9 ^c	8.1 \pm 1.1
CD18 ^{-/-}	92.2 \pm 0.5	54.9 \pm 3.3	92.7 \pm 1.4	15.1 \pm 1.6
CD18 ^{-/-} CD62P ^{-/-}	25.1 \pm 2.8 ^b	14.0 \pm 2.8	12.0 \pm 3.4 ^b	1.0 \pm 0.3 ^b

^a All values expressed as mean \pm SE. FOV, field of view. CD18^{-/-} group ($P < 0.05$).

^d Per 180 μ m vessel segment.

^b Significantly different all other groups.

^c Significantly different from

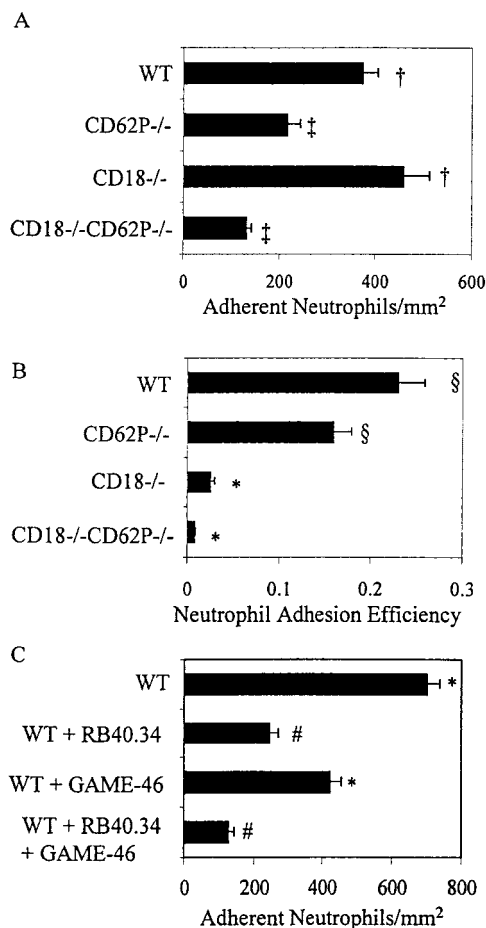


Figure 4. Neutrophil adhesion in TNF- α -treated cremaster muscle venules. *A*) The number of adherent leukocytes was obtained from venules during the 60 min after exteriorization of the cremaster muscle in wild-type, CD62P^{-/-}, CD18^{-/-}, and CD18^{-/-}CD62P^{-/-} mice and was expressed as adherent leukocytes per unit area. The number of adherent neutrophils was calculated by multiplying the neutrophil differential obtained from Giemsa-stained whole mounts (Table 2) by the leukocyte adhesion density obtained from intravital microscopy. *B*) Neutrophil adhesion efficiency was calculated by dividing the number of adhered neutrophils per unit area by the concentration of neutrophils in the systemic circulation to normalize neutrophil adhesion in mice that have significant differences in circulating neutrophil levels (Table 1). *C*) Neutrophil adhesion in wild-type mice with CD18 integrin and P-selectin function blocked. Wild-type mice were pre-treated with an anti-P-selectin mAb (RB40.34), an anti-CD18 mAb (GAME-46), or the anti-CD18 mAb and an anti-P-selectin mAb. To facilitate the counting of adherent leukocytes, all leukocyte rolling was blocked with an anti-E-selectin mAb (9A9) and/or the anti-P-selectin mAb 75 min after exteriorization of the cremaster muscle and the remaining adherent leukocytes were counted. The number of adhered neutrophils was calculated by multiplying the neutrophil differential obtained by histology (Table 3) with the leukocyte adhesion density obtained by intravital microscopy. *Significantly different from all other groups. †Significantly different from CD62P^{-/-} and CD18^{-/-}CD62P^{-/-} groups. ‡Significantly different from wild-type and CD18^{-/-} groups. §Significantly different from CD18^{-/-} and CD18^{-/-}CD62P^{-/-} groups. #Significantly different from wild-type and wild-type + GAME-46 groups ($P < 0.05$).

lung tissue, with concurrent hemorrhage and exudate (Fig. 5J). Bacterial colonization was evident in some fields and confirmed by bacterial cultures (Table 4). The lung septa were clearly visible in wild-type (Fig. 5F), CD18^{+/-}CD62P^{-/-} (Fig. 5G), and CD18^{-/-} (Fig. 5H) mice. Wild-type and CD18^{+/-}CD62P^{-/-} mice showed only a few neutrophils and mononuclear cells in the interstitium. Consistent with neutrophilia, CD18^{-/-} mice showed elevated levels of neutrophils in the lung interstitium; however, the amount of neutrophils in the lungs of CD18^{-/-} mice was dramatically less than that in age-matched CD18^{-/-}CD62P^{-/-} mice (compare Fig. 5H and I).

CD18^{-/-}CD62P^{-/-} mice displayed increased numbers of plasma cells in liver lesions not seen in wild-type, CD62P^{-/-}, or CD18^{-/-} mice. Some CD18^{-/-}CD62P^{-/-} mice showed neutrophil-containing microabscesses in the liver (Fig. 5K, L). Many CD18^{-/-}CD62P^{-/-} mice showed multifocal clusters of spindle-shaped cells associated with the sinusoids (Fig. 5J). Although the origin of these cells is uncertain, they appear to be associated with a chronic inflammatory process. CD18^{-/-}CD62P^{-/-} mice did not show alterations in kidney, heart, or gut architecture (data not shown).

Microbiological cultures

To investigate possible causes of early lethality in CD18^{-/-}CD62P^{-/-} mice, liver, lung, and spleen samples were analyzed for bacterial growth. No positive cultures were obtained in wild-type or CD62P^{-/-} mice (Table 4). Only one of nine CD18^{-/-} mice showed bacteria growth in the lung and liver (Table 4). Remarkably, 12 of 16 CD18^{-/-}CD62P^{-/-} mice showed bacterial growth in one or more of the organs tested (Table 4). Positive cultures were obtained from apparently healthy CD18^{-/-}CD62P^{-/-} mice as well as CD18^{-/-}CD62P^{-/-} mice showing symptoms of illness, such as drastic weight loss and a hunched posture (Fig. 1C). *Escherichia coli*, *Lactobacillus*, alpha-hemolytic *Streptococcus*, and/or *Streptococcus bovis* were cultured from 4 of 14 spleens, 10 of 16 livers, and 10 of 16 lung samples from CD18^{-/-}CD62P^{-/-} mice (Table 4), showing that CD18^{-/-}CD62P^{-/-} mice are highly susceptible to infection by fecal and commensal bacteria.

DISCUSSION

Although overtly healthy and indistinguishable from littermates through weaning, mice lacking CD18 integrins and P-selectin stop growing past 5 wk and show a distinctly severe phenotype and reduced viability in adulthood, usually not surviving longer than 6 months. Using intravital microscopy, we show that despite near-normal levels of general leukocyte rolling and adhesion, neutrophil recruitment is severely suppressed in these mice. Concomitantly, these mice are highly susceptible to bacterial colonization of the lung, liver, and

TABLE 3. Intravascular and transmigrated leukocyte differentials after TNF- α treatment^a

	Wild-type	Wild-type + RB40.34	Wild-type + GAME-46	Wild-type + RB40.34 + GAME-46
Intravascular differential				
% PMN	75 \pm 2	60 \pm 4	78 \pm 3	35 \pm 4 ^b
Transmigrated differential				
% PMN	87 \pm 4	44 \pm 7 ^b	68 \pm 5 ^c	25 \pm 4 ^b

^a All values expressed as mean \pm SE. ^b Significantly different from all other groups. ^c Significantly different from wild-type + RB40.34 and wild-type + RB40.34 + GAME-46 groups ($P < 0.05$).

spleen. The most important result of this study is the significant defect of neutrophil recruitment in CD18^{-/-} CD62P^{-/-} mice despite near-normal levels of leukocyte rolling and preserved slow rolling, indicating a role

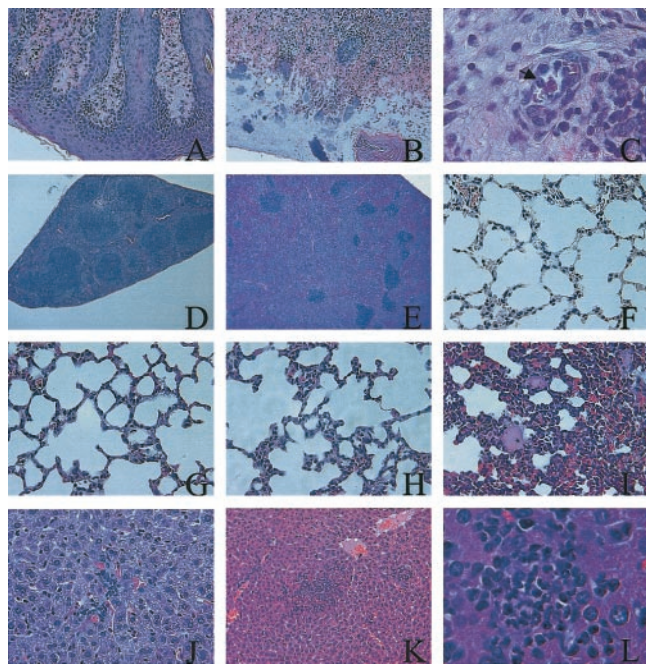


Figure 5. Histopathology of CD18^{-/-}CD62P^{-/-} double mutant mice. *A*) Epidermis in unaffected skin adjacent to the lesion. *B*) Necrosis of the epidermis in sections of skin displaying ulcerative dermatitis. *C*) The dermal inflammatory infiltrate consists of lymphocytes, mast cells, and plasma cells, and few neutrophils. Arrow shows an intravascular neutrophil. The spleen in CD18^{-/-}CD62P^{-/-} mice shows dramatic hyperplasia of the red pulp and increase in spleen size (*E*). Very few sections of white pulp remain in CD18^{-/-}CD62P^{-/-} mice compared with wild-type mice (*D*). Airways and alveolar spaces appear normal in wild-type (*F*), CD18^{+/+}CD62P^{-/-} (*G*), and CD18^{-/-} (*H*) mice. CD18^{-/-} mice show increased neutrophil accumulation in interstitial regions, consistent with neutrophilia in these mice. CD18^{-/-}CD62P^{-/-} mice show significant neutrophil accumulation, resulting in expanded interstitial regions and collapse of airway spaces (*I*). Liver samples from wild-type, CD18^{+/+}CD62P^{-/-}, and CD18^{-/-} mice appeared normal (not shown). In contrast, CD18^{-/-}CD62P^{-/-} mice show increased numbers of plasma cells and liver lesions consisting of microabscesses containing neutrophils (*K*, *L*) and multifocal clusters of spindle-shaped cells associated with the sinusoids (*J*). Samples depicted obtained from 3.5-month-old mice. Original magnification 10 \times (*A*, *B*, *K*), 40 \times (*F*-*J*), 4 \times (*D*, *E*), 100 \times (*C*, *L*).

of P-selectin in the CD18-independent neutrophil adhesion pathway.

Neutrophil recruitment is significantly restricted in some models of inflammation in the skin, in the lung, and in ischemic reperfusion injury when CD18 integrin function is blocked (22–26). However, no defect in neutrophil recruitment is seen in the absence of CD18 integrin function in other models of inflammation in the lungs, joints, and the peritoneal cavity, presumably because CD18-independent neutrophil recruitment pathways are up-regulated under certain inflammatory conditions (25, 27–30). Neutrophil recruitment levels in CD18^{-/-} mice are similar to those in wild-type mice in a 2 h TNF- α -induced model of inflammation (9), indicating that CD18-independent mechanisms can mediate efficient neutrophil recruitment in this inflammatory model. If unchallenged, many CD18^{-/-} mice remain healthy under barrier housing conditions, although some develop spontaneous skin lesions (15).

Remarkably, despite circulating neutrophil levels similar to CD18^{-/-} mice, CD18^{-/-}CD62P^{-/-} mice showed almost a complete absence of neutrophil recruitment in the 2 h TNF- α -induced model of inflammation. However, the mechanism underlying the severe neutrophil recruitment defect seems to be different from that in CD18^{-/-}CD62E^{-/-} mice. Mice deficient in CD18 integrins and E-selectin have drastically elevated leukocyte rolling velocities and lack slow leukocyte rolling (<10 μ m/s) (10). Reduced neutrophil adhesion in CD18^{-/-}CD62E^{-/-} mice is attributed to the lack of this slow rolling event, which appears to be critical for transition to firm adhesion. CD18^{-/-}CD62P^{-/-} mice have leukocyte rolling velocities similar to CD18^{-/-} mice, with many leukocytes rolling < 10 μ m/s (38%), but neutrophil recruitment is severely impaired in CD18^{-/-}CD62P^{-/-} mice compared with CD18^{-/-} mice. The curtailed neutrophil recruitment in CD18^{-/-}P^{-/-} mice does not result from a lack of slow rolling leukocytes, but rather a lack of transition from slow rolling to firm adhesion. This suggests that slowly rolling neutrophils require P-selectin ligation to transition to CD18-independent firm adhesion. Recently, ligation of PSGL-1, the major P-selectin ligand, has been shown to promote expression of various gene products in neutrophils and monocytes (31, 32). Such signaling events may be required for CD18-independent neutrophil adhesion.

CD18^{-/-} but not CD62P^{-/-} single mutant mice develop chronic dermatitis with extensive facial and sub-

TABLE 4. Microbiological analysis

	Spleen	Liver	Lung	Organisms cultured (number of times obtained)
Wild-type	0/9 ^a	0/9	0/9	na
CD62P ^{-/-}	0/4	0/7	0/7	na
CD18 ^{-/-}	0/5	1/9	1/9	alpha-hemolytic <i>Streptococcus</i> (2)
CD18 ^{-/-} CD62P ^{-/-}	4/14	10/16	10/16	<i>E. coli</i> (15), <i>Strep. Bovis</i> (2), <i>Lactobacillus</i> (2), alpha-hemolytic <i>Streptococcus</i> (5)

^a Positive cultures/total cultures taken.

mandibular erosions, although bacterial cultures from these skin sites are generally negative (15, 16). CD18^{-/-}CD62P^{-/-} share this phenotype with CD18^{-/-} mice. However, unlike CD18^{-/-} mice, CD18^{-/-}CD62P^{-/-} mice show positive bacterial cultures in major organs with fecal and commensal bacteria. Our data show that elimination of CD18 integrins and P-selectin severely impairs the ability to control normal flora-induced infections. In mice, P-selectin is more important for leukocyte rolling and adhesion than in humans (33, 34). The phenotype of CD18 null mice is less severe than that of patients with the severe form of leukocyte adhesion deficiency (35). The severe phenotype, normal flora-dependent infections, and premature death of CD18^{-/-}CD62P^{-/-} mice suggest that these mice may represent a model of severe leukocyte adhesion deficiency.

The substantial neutrophil infiltrate in the lungs and the liver of CD18^{-/-}CD62P^{-/-} mice shows CD18- and P-selectin-independent neutrophil recruitment to these organs. Several previous studies have suggested that neutrophil recruitment to the lung (25, 36–42) and liver (43, 44) does not require CD18 integrins. Similarly, neutrophils can enter the lung (45–47) and liver (48–50) in the absence of P-selectin. Most of these studies were done in mice challenged with an inflammatory stimulus. Our study is the first to show neutrophil accumulation in the lungs and livers of unchallenged CD18^{-/-}CD62P^{-/-} mice under vivarium conditions. Evidently, the mechanisms responsible for neutrophil recruitment to the lung and liver are fully preserved or even enhanced in the absence of CD18 and P-selectin. The severe lung pathology as well as the bacterial colonization of major organs may well contribute to the premature demise of CD18^{-/-}CD62P^{-/-} mice.

In conclusion, we show that mice lacking both CD18 integrins and P-selectin have severely reduced viability and impaired neutrophil adhesion despite significant levels of leukocyte rolling at slow velocities. Our data suggest that P-selectin-mediated rolling is mandatory for host defense in the absence of CD18 integrins. Our data also reveal significant differences in the impact of removing CD18 integrins and P-selectin on neutrophil recruitment to different organs. **[F]**

We thank Dr. A. L. Beaudet (Baylor College of Medicine, Houston, TX) for CD18^{-/-} mice. We also thank Jim White for genotyping mice and Michele Kirkpatrick for animal husbandry. This work was supported by National Institutes of Health grants HL54136 to K.L. and NRSA-HL10447 to S.B.F.

REFERENCES

- Butcher, E. C. (1991) Leukocyte-endothelial cell recognition: three (or more) steps to specificity and diversity. *Cell* **67**, 1033–1036
- Kansas, G. S. (1996) Selectins and their ligands: current concepts and controversies. *Blood* **88**, 3259–3287
- Hafezi-Moghadam, A., Thomas, K. L., Prorock, A. J., Huo, Y., and Ley, K. (2001) L-selectin shedding regulates leukocyte recruitment. *J. Exp. Med.* **193**, 863–872
- Smolen, J. E., Petersen, T. K., Koch, C., O'Keefe, S. J., Hanlon, W. A., Seo, S., Pearson, D., Fossett, M. C., and Simon, S. I. (2000) L-selectin signaling of neutrophil adhesion and degradation involves p38 mitogen-activated protein kinase. *J. Biol. Chem.* **275**, 15876–15884
- Steeber, D. A., Engel, P., Miller, A. S., Sheetz, M. P., and Tedder, T. F. (1997) Ligation of L-selectin through conserved regions within the lectin domain activates signal transduction pathways and integrin function in human, mouse, and rat leukocytes. *J. Immunol.* **159**, 952–963
- Gopalan, P. K., Smith, C. W., Lu, H., Berg, E. L., McIntire, L. V., and Simon, S. I. (1997) Neutrophil CD18-dependent arrest on intercellular adhesion molecule 1 (ICAM-1) in shear flow can be activated through L-selectin. *J. Immunol.* **158**, 367–375
- Kunkel, E. J., Dunne, J. L., and Ley, K. (2000) Leukocyte arrest during cytokine-dependent inflammation in vivo. *J. Immunol.* **164**, 3301–3308
- Ley, K. (2001) Pathways and bottlenecks in the web of inflammatory adhesion molecules and chemoattractants. *Immunol. Res.* **24**, 87–95
- Jung, U., Norman, K. E., Scharffetter-Kochanek, K., Beaudet, A. L., and Ley, K. (1998) Transit time of leukocytes rolling through venules controls cytokine-induced inflammatory cell recruitment in vivo. *J. Clin. Invest.* **102**, 1526–1533
- Forlow, S. B., White, E. J., Barlow, S. C., Feldman, S. H., Lu, H., Bagby, G. J., Beaudet, A. L., Bullard, D. C., and Ley, K. (2000) Severe inflammatory defect and reduced viability in CD18 and E-selectin double mutant mice. *J. Clin. Invest.* **106**, 1457–1466
- Moore, K. L., Stults, N. L., Diaz, S., Smith, D. F., Cummings, R. D., Varki, A., and McEver, R. P. (1992) Identification of a specific glycoprotein ligand for P-selectin (CD62) on myeloid cells. *J. Cell Biol.* **118**, 445–456
- Sako, D., Chang, X. J., Barone, K. M., Vachino, G., White, H. M., Shaw, G., Veldman, G. M., Bean, K. M., Ahern, T. J., and Furie, B. (1993) Expression cloning of a functional glycoprotein ligand for P-selectin. *Cell* **75**, 1179–1186
- Yang, J., Hirata, T., Croce, K., Merrill-Skoloff, G., Tchernychev, B., Williams, E., Flaumenhaft, R., Furie, B. C., and Furie, B. (1999) Targeted gene disruption demonstrates that P-selectin glycoprotein ligand 1 (PSGL-1) is required for P-selectin-mediated but not E-selectin-mediated neutrophil rolling and migration. *J. Exp. Med.* **190**, 1769–1782
- Robinson, S. D., Frenette, P. S., Rayburn, H., Cumiskey, M., Ullman-Cullere, M., Wagner, D. D., and Hynes, R. O. (1999) Multiple, targeted deficiencies in selectins reveal a predominant role for P-selectin in leukocyte recruitment. *Proc. Natl. Acad. Sci. USA* **96**, 11452–11457
- Scharffetter-Kochanek, K., Lu, H., Norman, K., van Nood, N., Munoz, F., Grabbe, S., McArthur, M., Lorenzo, I., Kaplan, S., Ley, K., Smith, C. W., Montgomery, C. A., Rich, S., and Beaudet, A. L. (1998) Spontaneous skin ulceration and defective T cell function in CD18 null mice. *J. Exp. Med.* **188**, 119–131

16. Bullard, D. C., Kunkel, E. J., Kubo, H., Hicks, M. J., Lorenzo, I., Doyle, N. A., Doerschuk, C. M., Ley, K., and Beaudet, A. L. (1996) Infectious susceptibility and severe deficiency of leukocyte rolling and recruitment in E-selectin and P-selectin double mutant mice. *J. Exp. Med.* **183**, 2329–2336
17. Jung, U., and Ley, K. (1999) Mice lacking two or all three selectins demonstrate overlapping and distinct functions for each selectin. *J. Immunol.* **162**, 6755–6762
18. Bosse, R., and Vestweber, D. (1994) Only simultaneous blocking of the L- and P-selectin completely inhibits neutrophil migration into mouse peritoneum. *Eur. J. Immunol.* **24**, 3019–3024
19. Norton, C. R., Rumberger, J. M., Burns, D. K., and Wolitzky, B. A. (1993) Characterization of murine E-selectin expression in vitro using novel anti-mouse E-selectin monoclonal antibodies. *Biochem. Biophys. Res. Commun.* **195**, 250–258
20. Pries, A. R. (1988) A versatile video image analysis system for microcirculatory research. *Int. J. Microcirc. Clin. Exp.* **7**, 327–345
21. Norman, K. E. (2001) An effective and economical solution for digitizing and analysing video-recordings of the microcirculation. *Microcirculation* **8**, 243–249
22. Price, T. H., Beatty, P. G., and Corpuz, S. R. (1987) In vivo inhibition of neutrophil function in the rabbit using monoclonal antibody to CD18. *J. Immunol.* **139**, 4174–4177
23. Nourshargh, S., Rampart, M., Hellewell, P. G., Jose, P. J., Harlan, J. M., Edwards, A. J., and Williams, T. J. (1989) Accumulation of ¹¹¹In-neutrophils in rabbit skin in allergic and non-allergic inflammatory reactions in vivo. Inhibition by neutrophil pretreatment in vitro with a monoclonal antibody recognizing the CD18 antigen. *J. Immunol.* **142**, 3193–3198
24. Issekutz, A. C., and Issekutz, T. B. (1992) The contribution of LFA-1 (CD11a/CD18) and MAC-1 (CD11b/CD18) to the in vivo migration of polymorphonuclear leukocytes to inflammatory reactions in the rat. *Immunology* **76**, 655–661
25. Doerschuk, C. M., Winn, R. K., Coxson, H. O., and Harlan, J. M. (1990) CD18-dependent and -independent mechanisms of neutrophil emigration in the pulmonary and systemic microcirculation of rabbits. *J. Immunol.* **144**, 2327–2333
26. Vedder, N. B., Winn, R. K., Rice, C. L., Chi, E. Y., Arfors, K. E., and Harlan, J. M. (1990) Inhibition of leukocyte adherence by anti-CD18 monoclonal antibody attenuates reperfusion injury in the rabbit ear. *Proc. Natl. Acad. Sci. USA* **87**, 2643–2646
27. Winn, R. K., and Harlan, J. M. (1993) CD18-independent neutrophil and mononuclear leukocyte emigration into the peritoneum of rabbits. *J. Clin. Invest.* **92**, 1168–1173
28. Issekutz, A. C., and Issekutz, T. B. (1993) A major portion of polymorphonuclear leukocyte and T lymphocyte migration to arthritic joints in the rat is via LFA-1/MAC-1-independent mechanisms. *Clin. Immunol. Immunopathol.* **67**, 257–263
29. Mizgerd, J. P., Kubo, H., Kutkoski, G. J., Bhagwan, S. D., Scharffetter-Kochanek, K., Beaudet, A. L., and Doerschuk, C. M. (1997) Neutrophil emigration in the skin, lungs, and peritoneum: different requirements for CD11/CD18 revealed by CD18-deficient mice. *J. Exp. Med.* **186**, 1357–1364
30. Doerschuk, C. M., Tasaka, S., and Wang, Q. (2000) CD11/CD18-dependent and -independent neutrophil emigration in the lungs: how do neutrophils know which route to take? *Am. J. Respir. Cell Mol. Biol.* **23**, 133–136
31. Hidari, K. I., Weyrich, A. S., Zimmerman, G. A., and McEver, R. P. (1997) Engagement of P-selectin glycoprotein ligand-1 enhances tyrosine phosphorylation and activates mitogen-activated protein kinases in human neutrophils. *J. Biol. Chem.* **272**, 28750–28756
32. Mahoney, T. S., Weyrich, A. S., Dixon, D. A., McIntyre, T., Prescott, S. M., and Zimmerman, G. A. (2001) Cell adhesion regulates gene expression at translational checkpoints in human myeloid leukocytes. *Proc. Natl. Acad. Sci. USA* **98**, 10284–10289
33. Pan, J., Xia, L., Yao, L., and McEver, R. P. (1998) Tumor necrosis factor- α - or lipopolysaccharide-induced expression of the murine P-selectin gene in endothelial cells involves novel kappaB sites and a variant activating transcription factor/cAMP response element. *J. Biol. Chem.* **273**, 10068–10077
34. Pan, J., Xia, L., and McEver, R. P. (1998) Comparison of promoters for the murine and human P-selectin genes suggests species-specific and conserved mechanisms for transcriptional regulation in endothelial cells. *J. Biol. Chem.* **273**, 10058–10067
35. Bunting, M., Harris, E. S., McIntyre, T. M., Prescott, S. M., and Zimmerman, G. A. (2002) Leukocyte adhesion deficiency syndromes: adhesion and tethering defects involving beta 2 integrins and selectin ligands. *Curr. Opin. Hematol.* **9**, 30–35
36. Hellewell, P. G., Young, S. K., Henson, P. M., and Worthen, G. S. (1994) Disparate role of the beta 2-integrin CD18 in the local accumulation of neutrophils in pulmonary and cutaneous inflammation in the rabbit. *Am. J. Respir. Cell Mol. Biol.* **10**, 391–398
37. Qin, L., Quinlan, W. M., Doyle, N. A., Graham, L., Sligh, J. E., Takei, F., Beaudet, A. L., and Doerschuk, C. M. (1996) The roles of CD11/CD18 and ICAM-1 in acute *Pseudomonas aeruginosa*-induced pneumonia in mice. *J. Immunol.* **157**, 5016–5021
38. Ramamoorthy, C., Sasaki, S. S., Su, D. L., Sharar, S. R., Harlan, J. M., and Winn, R. K. (1997) CD18 adhesion blockade decreases bacterial clearance and neutrophil recruitment after intrapulmonary *E. coli*, but not after *S. aureus*. *J. Leukoc. Biol.* **61**, 167–172
39. Motosugi, H., Quinlan, W. M., Bree, M., and Doerschuk, C. M. (1998) Role of CD11b in focal acid-induced pneumonia and contralateral lung injury in rats. *Am. J. Respir. Crit. Care Med.* **157**, 192–198
40. Sherman, M. P., Johnson, J. T., Rothlein, R., Hughes, B. J., Smith, C. W., and Anderson, D. C. (1992) Role of pulmonary phagocytes in host defense against group B streptococci in preterm versus term rabbit lung. *J. Infect. Dis.* **166**, 818–826
41. Keeney, S. E., Mathews, M. J., Haque, A. K., Rudloff, H. E., and Schmalstieg, F. C. (1994) Oxygen-induced lung injury in the guinea pig proceeds through CD18-independent mechanisms. *Am. J. Respir. Crit. Care Med.* **149**, 311–319
42. Mulligan, M. S., Wilson, G. P., Todd, R. F., Smith, C. W., Anderson, D. C., Varani, J., Issekutz, T. B., Miyasaka, M., and Tamatani, T. (1993) Role of beta 1, beta 2 integrins and ICAM-1 in lung injury after deposition of IgG and IgA immune complexes. *J. Immunol.* **150**, 2407–2417
43. Lawson, J. A., Farhood, A., Hopper, R. D., Bajt, M. L., and Jaeschke, H. (2000) The hepatic inflammatory response after acetaminophen overdose: role of neutrophils. *Toxicol. Sci.* **54**, 509–516
44. Jaeschke, H., Farhood, A., Fisher, M. A., and Smith, C. W. (1996) Sequestration of neutrophils in the hepatic vasculature during endotoxemia is independent of beta 2 integrins and intercellular adhesion molecule-1. *Shock* **6**, 351–356
45. Sharar, S. R., Chapman, N. N., Flaherty, L. C., Harlan, J. M., Tedder, T. F., and Winn, R. K. (1996) L-selectin (CD62L) blockade does not impair peritoneal neutrophil emigration or subcutaneous host defense to bacteria in rabbits. *J. Immunol.* **157**, 2555–2563
46. Mulligan, M. S., Watson, S. R., Fennie, C., and Ward, P. A. (1993) Protective effects of selectin chimeras in neutrophil-mediated lung injury. *J. Immunol.* **151**, 6410–6417
47. Wickel, D. J., Mercer-Jones, M., Peyton, J. C., Shrotri, M. S., and Cheadle, W. G. (1998) Neutrophil migration into the peritoneum is P-selectin dependent, but sequestration in lungs is selectin independent during peritonitis. *Shock* **10**, 265–269
48. Shi, J., Kokubo, Y., and Wake, K. (1998) Expression of P-selectin on hepatic endothelia and platelets promoting neutrophil removal by liver macrophages. *Blood* **92**, 520–528
49. Essani, N. A., Fisher, M. A., Simmons, C. A., Hoover, J. L., Farhood, A., and Jaeschke, H. (1998) Increased P-selectin gene expression in the liver vasculature and its role in the pathophysiology of neutrophil-induced liver injury in murine endotoxin shock. *J. Leukoc. Biol.* **63**, 288–296
50. Kamochi, M., Kamochi, F., Kim, Y. B., Sawh, S., Sanders, J. M., Sarembock, I., Green, S., Young, J. S., Ley, K., Fu, S. M., and Rose, C. E., Jr. (1999) P-selectin and ICAM-1 mediate endotoxin-induced neutrophil recruitment and injury to the lung and liver. *Am. J. Physiol.* **277**, L310–L319

Received for publication March 21, 2002.

Accepted for publication June 25, 2002.